PROGRESSIVE DAMAGE ANALYSIS OF TOW-STEERED COMPOSITE PANELS IN POSTBUCKLING

Cláudio S. Lopes[1,2], Pedro P. Camanho[1], Zafer Gürdal[2], Brian F. Tatting[3]
[Claudio S. Lopes]: C.S.FariaLopes@tudelft.nl
[1]University of Porto, Portugal [2]Delft University of Technology, The Netherlands
[3]ADOPTECH, Inc., Virginia, USA

Keywords: *Tow-Steered Composites, Tow-Placement, Damage, Failure, Strength*

Abstract

Machines capable of individually controlling fibre tows and placing them onto the surface of a laminate with curvilinear topology are available nowadays. Due to the variation of properties along their surface, such structures are termed variable-stiffness composite panels.

Experimental research demonstrated that properly designed tow-steered panels buckle at higher loads than traditional straight-fibre laminates. Also, numerical analyses by the authors demonstrated that first-ply failure of these designs is remarkably postponed. The focus of this paper is to extend those analyses into the postbuckling progressive damage behaviour and final structural failure. A user-developed continuum damage model implemented in the finite element code ABAQUS® is employed in the characterisation of damage initiation and propagation.

As with damage initiation, failure of curvilinear-fibre panels is remarkably postponed as compared with straight-fibre laminates. Tow-steered panels also show to be more tolerant to notches than traditional laminates. By taking into account the residual thermal stresses, not only predicted and experimented buckling loads show remarkable agreement but also predicted final failure loads of tow-steered panels in postbuckling are within 12% of the experimental results.

1 Introduction

During the last decade an innovative composite manufacturing technology was developed. By combining features of automated tape laying and filament winding, automated tow-placement machines are capable of economically producing a wide range of high-quality composite products. Furthermore, tow-placement technology expands the range of manufacturable laminate designs by allowing fibre-tows to be steered throughout each lamina. Since the fibre orientation defines the stiffness (and many of the intrinsic) properties of a laminate, composite panels with in-plane variations of the fibre angle were termed *variable stiffness panels* (Fig. 1). These panels demonstrated great potential for improving the structural performance of composite structures in terms of stiffness, buckling, and failure loads.

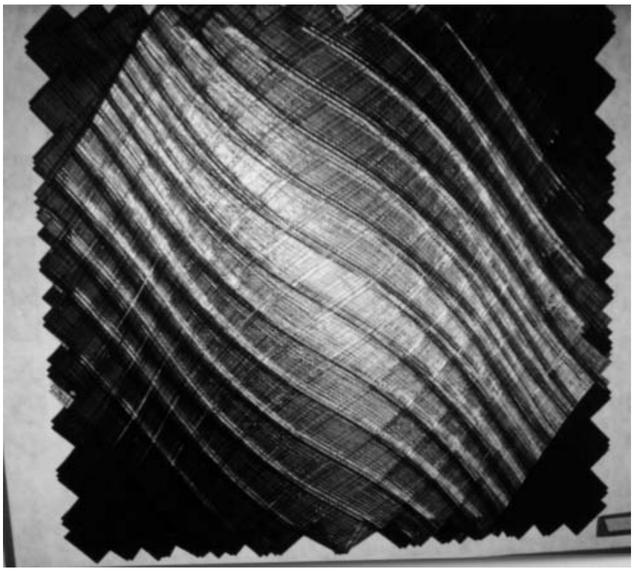

Fig. 1. Example of a tow-steered panel

In an effort to integrate realistic fabrication techniques into the design of laminates with curvilinear fibre layers, research carried out by Gürdal et al. [1],[2] introduced fibre path definitions, formulated closed-form and numerical solutions for simple rectangular plates. Promising results in terms of stiffness and buckling generated by analytical and numerical research were achieved [3],[4]. Several panels were fabricated to validate the manufacturability of tow-steered laminates [5]. Subsequent testing by Wu et al. [6] confirmed the increased load-carrying capability of variable-stiffness panels over traditional straight-fibre designs.

Tow steered ply definitions can formulated with a small number of parameters. These parameters define a reference course for the tow-placement head. The remainder of the ply is constructed by shifting this reference path as many times as needed for its complete coverage. To prevent the overlap regions, the tow placement machine can also be instructed to cut tows individually so that no thickness builds up. This method is referred to as the *tow-drop method*, in opposition to the *overlap method* shown in Fig. 1. It results in constant thickness panels that contain small wedge-like areas free of fibres due to the dropping of tows.

So far, failure analyses have been performed in the design of tow-steered laminates by using criteria based on curve-fitting techniques, with the only purpose of guaranteeing that first-ply failure occurs well after the first buckling mode [7],[8]. The present authors carried first-ply failure analyses [9] on variable-stiffness panels optimised for buckling, by using the set of phenomenological failure criteria LaRC04 developed at NASA Langley Research Centre [10]. According to the numerical solutions, tow-steered panels showed improvements as great as 34% when compared with classical straight-fibre laminates.

The objective of this paper is to extend the previous analyses into the complete progressive damage and final failure processes of variable-stiffness laminates loaded in compression, and compare their performance with traditional laminates. The material model used in this research was developed by Maimí et al. [11] and is based on Continuum Damage Mechanics (CDM), a methodology well suited for the simulation of damage evolution and ultimate failure of composite structures.

2 Progressive Damage and Failure Analyses

The ability to predict the initiation and growth of damage in fibre reinforced plastic structures is essential to evaluate their performance and to develop reliable and safe designs which exploit the advantages offered by composites. Since most composite materials exhibit quasi-brittle failure, with little or no margin of safety through ductility as offered by many metals, the propagation damage mechanisms in composite structures must be understood.

Under normal operating conditions, laminated composite structures can exhibit local damage mechanisms such as matrix cracks, fibre breakage, fibre-matrix debonding and delaminations which contribute to final failure. Strength-based failure criteria are commonly used to predict these phenomena. A large number of continuum-based criteria have been derived to relate stresses and experimental measures of material strength to the onset of failure [10]. However, for most of the cases failure criteria can only predict the onset of the different damage mechanisms occurring in composite materials. For composite structures that can accumulate damage before structural collapse, the use of failure criteria is not sufficient to predict ultimate structural failure. To bridge this gap, the past recent years have seen the development of numerical methodologies to address the progressive failure of composite materials [12].

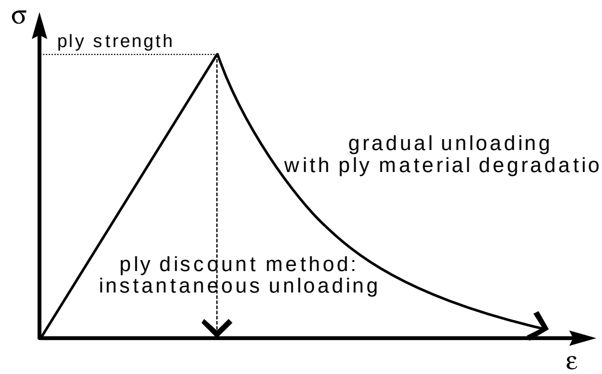

Fig. 2 Idealised damage behaviours in composite laminates.

The simplest damage model for laminated composites is the ply discount: when first-ply failure is detected the whole stiffness of the lamina is removed from the laminate stiffness matrix, as illustrated in Fig. 2. This method, and other simplified methods, can be used to get rough estimates of the final failure of a composite structure. However, continuum damage mechanics is a more accurate methodology to predict the quasi-brittle failure of composites. In this way, the more realistic gradual unloading of a ply after the onset of damage is simulated by means of a material degradation model (Fig. 2).

Non-linear constitutive models defined in the context of the mechanics of continuum mediums have been developed and implemented in finite element codes in recent years. A continuum damage model, developed by Maimí et al. [11], for the prediction of damage onset and structural collapse of structures manufactured of fibre-reinforced plastic laminates is used in this work. Damage activation functions based on the LaRC04 failure criteria [10] are implemented in the model to predict the distinct damage mechanisms occurring at the ply level.

3 Panel Failure in Postbuckling

The implementation of the continuum damage model in ABAQUS® allows the numerical analysis of progressive failure of composite structures, in particular of variable-stiffness panels. In this work, such capability is used to compare the postbuckling strength of panels built with straight and steered fibres. Furthermore, the results of the simulations are compared with experimental data obtained by Jegley et al. [13],[14]. The effect of a circular central hole on the strength reduction of steered and non-steered composite panels is also studied.

3.1 Experimental set-up

The structures simulated consist of 20-layer composite panels (508x381*mm*) with and without central holes (D=76.2*mm*), loaded in compression, as illustrated in Fig. 3. In previous experiments on these panels [13],[14] the load was increased in the postbuckling regime until failure. End-shortening and out-of-plane displacements were measured by Direct Current Displacement Transducers (DCDT's) attached to the panels, as shown in Fig. 3. The advantages of tow-steered designs over straight-fibre designs were clearly demonstrated. Not only the buckling loads increased by up to a factor of 2 but also failure loads showed a maximum increase of 60%.

Three variants of the composite panel specimens are considered, corresponding to three construction methods: i) the straight-fibre method, ii) the fibre-steered method with dropped tows and iii) the fibre-steered method with overlapping tows. The layups chosen for the analysis were the ones previously determined by Tatting et al. [7],[8], based on buckling optimisation design. This optimisation was carried out only for the plates without holes. The same optimization results were assumed for the notched plates. For the straight-fibre configuration the best design was found to be the one with the stacking sequence $[\pm 45_2/\pm 30/\pm 45/\pm 15]_s$ whilst for the fibre-steered variants the best layup is $[\pm 45/\pm\langle 45|60\rangle_2/\pm\langle 30|15\rangle/\pm\langle 45|60\rangle]_s$. The external plies were constrained to the straight-fibre method to avoid visible gaps and overlaps. The tow-steered plies were staggered in order to disperse the tow-drops and reduce the laminate thickness variations. The thickness of each layer is 0.1397*mm*, which add up to 2.795*mm* thick laminates.

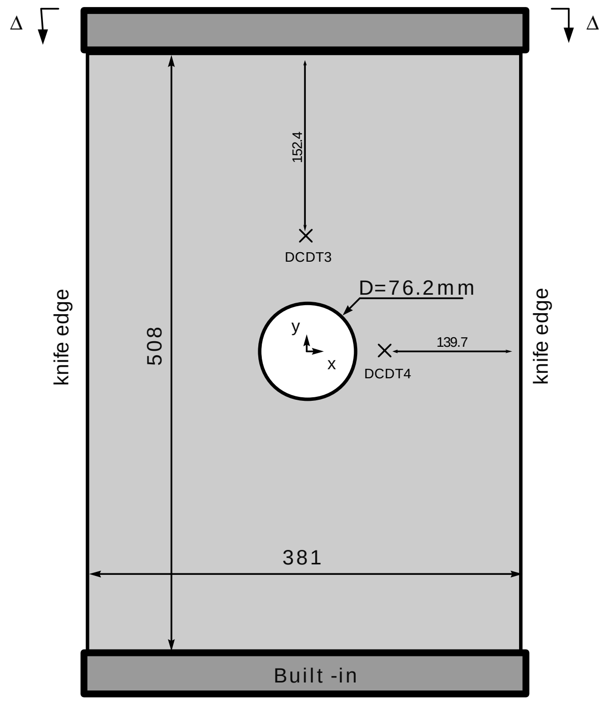

Fig. 3. Panel geometry and boundary conditions. Dimensions in *mm*.

3.2 Material Properties and In-situ effects

The panels tested were built with the epoxy-resin system AS4-9773. The elastic and strength properties for this material system are available in Table 1 and Table 2 [13][14].

Table 1. AS4/9773 elastic properties

E_1 (GPa)	E_2 (GPa)	G_{12} (GPa)	ν_{12}	α_1 (με/°C)	α_2 (με/°C)
129.8	9.2	5.1	0.36	-0.34	34.4

Table 2. AS4/9773 unidirectional strengths (MPa)

X^T	X^C	Y^T	Y^C	S^L
2070	1160	29.0	157.9	91.0

The continuum damage model implemented requires that the fracture energies corresponding to each failure mode are given as input. However, these properties are not available for the material AS4-9773, as only recently specific testing methods were devised to determine part of them [15]. An experimental programme to determine the fracture energies for the AS4-9773 system is out of the scope of this investigation. The material system IM7-8552 is found to be similar to the AS4-9773, as far as elastic and strength properties are concerned. Its fracture energies, shown in Table 3, were determined through in-house testing [15]. In this work they are used in place of the AS4-9773 system fracture energies.

Table 3. IM7/8552 fracture energies (N/mm)

G_2^+	G_6	G_2^-	G_1^+	G_1^-
0.28	0.79	1.31	27.5	106.3

The strength of a ply is a function of its thickness and location in the laminate. This effect, called the *in-situ effect* [16], significantly influences the strength of a ply when it is constrained by other plies with different fibre orientations. In other words, when evaluating the strength of a laminate, the unidirectional strength values of each lamina should be adjusted to take into account for its position within the laminate and the overall number of plies clustered together. The LaRC04 failure criteria take into account the in-situ effect characterised by higher transverse tensile and shear strengths of a ply when it is constrained by plies with different fibre orientations in a laminate, as compared with the strength of the same ply in a unidirectional laminate [16]. The in-situ transverse tensile and in-plane shear strengths follow from the respective critical energy release rate for crack propagation. The concept of interaction energy, which is defined as the energy released by the introduction of a crack in a ply subjected to in-plane transverse tensile and shear stresses, is used to calculate the individual components of the energy release rate from which the in-situ strengths are obtained [16].

2.3 FE implementation

The models simulate the boundary conditions used in the experiments are illustrated in Fig. 3. On the lower edge, the built-in condition is modelled by restraining all degrees of freedom. On the top edge, displacements are only allowed in the vertical direction. The load is introduced through an increasing compressive force at the top edge. Out-of-plane displacements and rotations about the horizontal direction are restrained at both side edges to simulate the effect of the knife edges in the experiments.

The FE meshes hold between 29224 (notched specimen) and 30858 (unnotched specimen) fully integrated *S4* shell elements, approximately 2.5x2.5*mm* in size, with 177726 and 187284 degrees-of-freedom, respectively for the notched and unnotched specimen. Such small elements are required for a correct representation of the dissipated energy.

The FE models were originally constructed using identical layups, where each element corresponded to a traditional straight fibre layup, i.e. each shell element in the model definition pointed to the same shell property entry card defined to specify the stacking sequence of the complete laminate. For curvilinear-fibre layers it is necessary to define a specific stacking sequence for each individual element according to the required variation of the fibre orientation angle. Depending on the fabrication method used, the local stacking sequence can be calculated for an arbitrary point in the panel and a generic FE model can be transformed into a tow steered design merely by re-defining the layup property entry, the ABAQUS® **Shell Section* card, for each element. This process has been automated through the development of a Java-based software tool termed *Laminate Definition Tool* (LDT) designed to re-define a flat laminate with the desired tow steered layup [17]. Therefore, for each element in the tow-steered FE models a unique **Shell Section* is created.

The LDT tool not only redefines the local fibre direction but, for the case of tow-overlapping designs, also updates the laminate thickness by stacking extra layers at the overlap locations. Therefore, the mass of tow-steered panels with overlapping tows slightly increases in comparison to its constant thickness counterparts. The extra mass is calculated to be 10.3% and 10.2% for the panels with and without hole, respectively.

One of the requirements imposed on the optimisation procedure carried out by Tatting et al. [7],[8] was that generated designs should fail at a reasonably higher load than the buckling load. This was verified using the Tsai-Wu first-ply failure criterion. Therefore, if damage and failure analyses are to be conducted on these panels they should contemplate the non-linear postbuckling phase. In order to generate the nonlinear solutions in the buckling path using ABAQUS®, a linear bifurcation analysis is performed in the first place and the first two buckling modes for the structure are calculated. Then, the FE model is re-defined with the buckling modes introduced as small initial imperfections with small magnitudes, as compared to the panel thickness (1-5%). Finally, geometric and material nonlinear solutions are determined for loads up to structural failure, as predicted by the implemented damage model. Panel inertia is taken into account by using a dynamic solution procedure. The problem is stabilised by the introduction of the mass matrix. The mode jumping phenomenon, where a significant part of the model strain energy is suddenly released, can be accurately predicted.

Residual thermal stresses resulting from the laminate curing process are simulated through application of thermal steps previous to the load bifurcation and the nonlinear dynamic loading steps. In these thermal steps a linear cool-down ($\Delta T=137.8^{\circ}C$) is enforced [5],[6].

The user-developed *FORTRAN* routine *UMAT*, which implements of the continuum damage model, runs for each of the four element integration points, at each equilibrium iteration. This routine can also handle thermal loading events. Each nonlinear analysis takes about 12 hours to complete using two state-of-the art CPU's in parallel processing and uses up to 3Gb of RAM.

4 Results, Comparison with the Experiments

In this chapter the results obtained through FE analyses on the composite panels with and without central hole are presented. These are compared with experimental data, when available. Since the analyses cover several structural phenomena such as buckling, damage and failure, the following explanation is divided accordingly.

4.1 Residual Thermal Stresses

During the curing process, stress-free laminates at an elevated temperature are gradually brought down to room temperature. Since the plies have different coefficients of thermal expansion in the longitudinal and transverse directions, a residual stress state is induced after curing the laminate. These residual stresses may have an important influence in the laminate failure process. Since during cool-down fibres tend to expand and matrix tends to shrink, the compressive loading range may be reduced in fibre direction and increased in the transverse direction. Also, for variable-stiffness panels, the thermal residual stresses are not uniform layerwise like they are for straight-fibre laminates. This generates non-zero section forces throughout the laminates which also influence the bifurcation loads besides further affecting the damage path. Therefore, the first step required for the correct analysis of the composite panels is the computation of the stress/displacement state resultant of the laminates curing process.

The straight-fibre panel shrinks in the longitudinal direction and expands in the width direction. This deformation is homogeneous in-plane, i.e. the edges remain straight after deformation. The tow-steered panel shrinks in both longitudinal and width directions but the deformation is not homogeneous. The non-homogeneity of the deformations in tow-steered panels due to curing is associated with the non-zero residual section forces shown in Fig. 4. Negative normal forces develop close to the edges of the panels while positive forces appear at the inside. These are beneficial in resisting buckling since the centre of the panel, by being unsupported, is the region that eventually triggers this phenomenon.

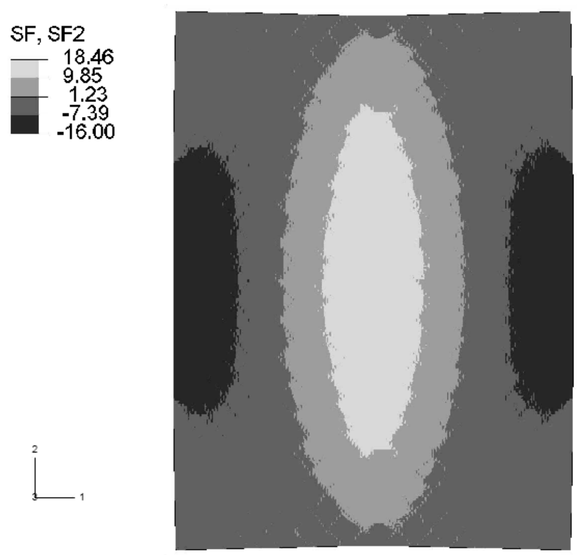

Fig. 4. Residual thermal section force N_y (N/mm)

4.2 Buckling

As observed experimentally, the unnotched panels when loaded under increasing compressive force, buckle in a half-wave pattern and remain on this buckling mode as the load increases up to structural failure of the panel. However, a central hole in panels of the same size and configuration triggers the change of buckling mode from half-wave to a full-wave pattern.

The bifurcation points, mode change behaviour and displacements can be analysed through the load-displacement curves plotted in Fig. 5. Taking as an example the straight-fibre panel under compression, out-of-plane displacements are not observed until the 1st bifurcation point is reached at a load level of 13858N.

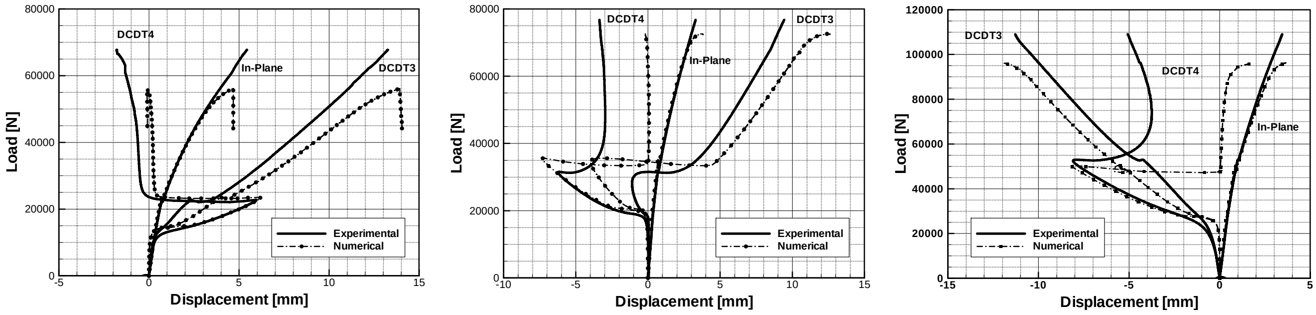

(a) Straight-fibres (b) Steered-fibres (w/ drops) (c) Steered-fibres (w/ overlaps)

Fig. 5. End-shortening and out-of-plane displacement curves for the panels with central holes.

As the panel buckles in half-wave pattern, the displacements measured by DCDT3 and DCDT4 grow in the same (positive) direction. Also, a decrease of structural stiffness is revealed by the end-shortening load-displacement curve. At 22771N the panel finds another equilibrium path by changing its shape to a full-wave buckle. The displacements measured by DCDT3 still evolve in the same direction but DCDT4 is taken to a slightly negative displacement path. The in-plane displacement curve shows a slight decrease in the load carrying capability of the panel between these two equilibrium states. This second buckling mode is maintained until the structure finally fails. For the remaining notched panels the behaviour is similar.

Fig. 5 also compares the displacements measured experimentally with the ones obtained numerically. There is a remarkable agreement between the end-shortening curves. However, the out-of-plane displacements observed in the experiments are replicated by FE analyses with less accuracy, mainly for the tow-steered panels.

According to the experimental results, the linear response range is extended by 42% for tow-steered laminates with dropped tows and 90.3% for the case of overlapping tows. Here, the extra mass of the steered laminates with overlapping tows is accounted for by mass-normalising the results.

In part, this beneficial effect can be attributed to the added capacity for load redistribution of tow-steered laminates, mainly the ones with overlapping tows, i.e. curvilinear fibre designs redirect load fluxes from the central regions of the panels to its edges. Since the edges are stiffer due to the prescribed boundary conditions, buckling of the structure is postponed to a higher applied load.
Another cause for higher buckling loads in tow-steered panels is the effect of induced thermal stresses. As explained before, curvilinear-fibre laminates develop in-plane thermal stresses during the curing process, resulting in tensile pre-stress regions in the centre of the panels. These remarkably improve the bifurcation loads. If no pre-stresses are taken into account in the analyses of these panels, the initial bifurcation loads are, on average under-predicted by 30%.

In addition, tow-overlaps generate the effect of "integral stiffeners" in the panel. This helps increasing buckling loads further.

By comparing the notched and unnotched panels, tow-steered panels seem to be more tolerant the hole. The effect of the notch is the reduction of the first bifurcation load by 11.5% in the case of straight-fibres and around 8.5% for the curvilinear-fibre panels.

4.3 Damage

By progressively increasing the compressive forces above the buckling loads, the growing stresses on the panels eventually lead to damage initiation and propagation at specific locations on some of the layers. This means that the combination of local longitudinal (fibre), transverse (matrix) and shear stresses is such that one, or more, damage initiation criteria are fulfilled. The outmost layers of the panels are prone to damage sooner than the inner ones due to two reasons. Due to the installed buckling mode, the panel deforms out-of-plane with increasing bending forces. As a result, the bending strains and stresses are higher in the outer layers of the panels: tension and compressive stresses are generated on the outer and inner side of the buckles, respectively. The second reason for premature damage is the reduced in-situ strength of the two outmost panel layers. As they become damaged and their load-carrying capability decreases, the load is transferred to the adjacent layers which also start to damage as a consequence of increased stress levels.

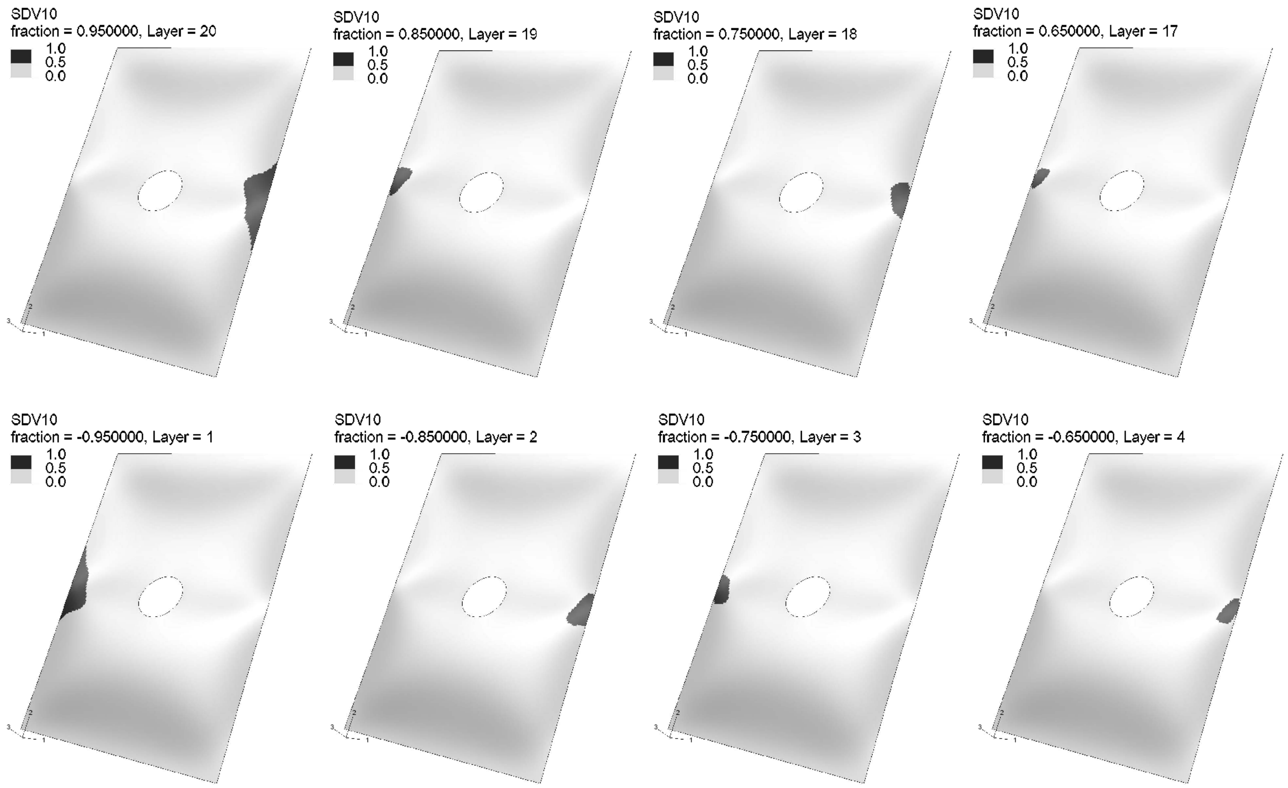

Fig. 6. Shear damage variable (d_6) on the four outmost layers at each (straight-fibre) notched panel side, at maximum load level. Note: Layer 1 has the lowest out-of-plane coordinate value.

Fibre stresses are by far the ones contributing most to the stress loading of the simulated composite panels. The level of fibre compression easily reaches 1.5GPa while the other in-plane stress components (σ_{22} and σ_{12}) are kept at an order of magnitude lower. This eventually leads to panel failure highly dominated by fibre kinking. Fig. 6 depicts the shear damage variable (d_6) at the four outmost layers at each side of the straight-fibre notched panels. Again, similar d_6 distributions develop for tow-steered panels. The shear-stiffness damage variable d_6 is affected by longitudinal and transverse cracks. In the present cases the influence of longitudinal (fibre) cracks is markedly greater than of transverse (matrix) cracks. The damage distributions confirm that the most damaged regions are the ones simultaneously in the outermost layers and loaded in compression.

The comparison of the damage response of the laminates built according to the three different construction methods is best done by analysing the damage initiation loads presented in Table 4. As expected, damage initiation is postponed to higher loads as the laminate construction method is changed from straight to steered fibres. The benefit is quite remarkable for panels with overlapping tows, for which damage is initiated at a 69.2% higher load level than its straight-fibre counterpart. This construction technique shows the added benefit of reducing the degrading influence of the hole on the panel elastic load range. For traditional straight-fibre panels and constant thickness tow-steered panels, the central hole causes the a decrease higher than 25% on the damage onset load. For curvilinear-fibre panels with tow-overlaps, this difference is cut to 16.8%. This beneficial effect can be attributed to the the "integral stiffeners" generated by overlapping tows which develop mostly outside the central region of the panel.

The damage load range, i.e. the load region corresponding to damage progression until final structural failure, is between 22 and 30% of the total panel load capacity. Although, the onset of damage occurs by fibre damage, matrix damage also occurs at a higher load level.

Table 4. Damage initiation results (notched panel).

Construction Method	Damage onset [kN]	Comparison [%]	Strength reduction due to the hole [%]
Straight	40.2	-	-25.1
Drops	55.0	36.8	-26.5
Overlaps	70.8	69.2	-16.8

4.4 Strength

Fig. 7 shows the load vs. end-shortening curves corresponding to the tested and simulated panels with central hole. Most of the simulations end at the maximum load level at which equilibrium is achieved. This is generally at the failure load level.

The load-displacement behaviour of the simulated notched panels compares remarkably well with the experimental results except at the end of the load path. The simulations predict a slight material softening while this behaviour was not observed in the experiments, i.e. the composite panels failed catastrophically without visible damage. This softening is coincident with the region where matrix damage occurs. Here, the fracture toughness properties used, mainly for the transverse direction, may be playing a role. The fracture energy for the 977-3 resin, from which the laminates are actually built from, may be significantly higher than for the 855-2 resin whose properties are used instead.

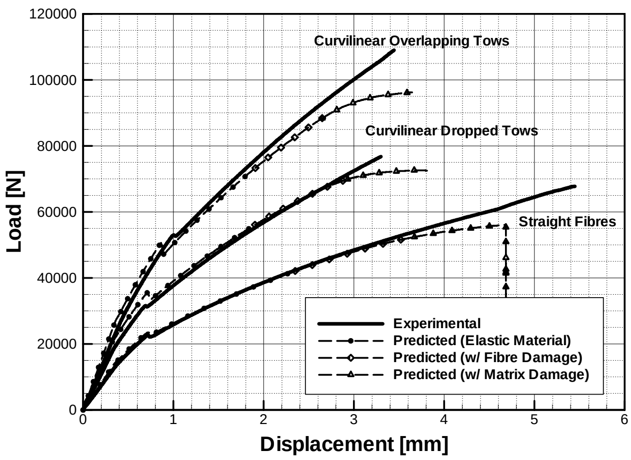

Fig. 7. Load vs. end-shortening curves for the simulated and tested notched panels. Hollow symbols identify damage progression

The failure loads are predicted to within 12% and 18% of the experimental results, for curvilinear and straight-fibre panels respectively. More remarkable is the accuracy on the prediction of the end-displacement levels at which failure occurs. It should be stressed here that the numerical results are being compared with one experimental result only. Scatter in the range of 10% and higher in failure tests of composites is no exception, i.e. average failure loads may differ substantially from the presented ones and may be more coherent with the numerical predictions.

Table 5 compares the results for the notched panel manufactured according to different construction methods. The beneficial effect on structural strength of steering fibre-tows within each lamina is remarkable. As with damage initiation, the greatest advantage (55.5%) is achieved with the tow-steered panel constructed by the tow-overlapping technique. Also here, the detrimental effect of the hole on panel strength is reduced from around 25% for constant thickness panels to 15.8% in the case of curvilinear-fibres and tow-overlaps.

Table 5 Strength results (notched panel).

C. Method	Strength (Exp.) [kN]	Strength (Num.) [kN]	Diff. [%]	Comp. [%]	Effect of the hole [%]
Straight	67.7	56.1	-17.1	-	-26.6
Drops	76.8	72.6	-5.5	13.4	-24.4
Overlaps	109.0	96.2	-11.7	55.5	-15.8

5 Conclusions

Progressive damage and failure analyses were conducted on panels with and without central holes, designed by the straight-fibre technique and innovative tow-steering methods. Known, through previous experimental testing, to increase the buckling loads as compared to traditional laminates, the damage behaviour and final structural collapse of curvilinear-fibre panels remained uncharacterised. The implementation of a continuum damage model in the commercially available code ABAQUS® allowed the correct simulation of the complete behaviour of composite panels when subjected to increasing compression loads.

The numerical results produced in this work show remarkable agreement with experimental data, both in terms of buckling loads and of final structural failure of tow-steered laminates. Laminates with curvilinear-fibre topology, mainly the ones in which fibre tows are allowed to overlap, show remarkable improvements on the retardation of damage initiation and on the increase of structural strength. In both indicators, the benefit is higher than 50%.

Variable-stiffness panels show a remarkable capacity for load redistribution, i.e. curvilinear fibre designs can redirect load fluxes from the central regions of panels to their stiffer edges, hence increasing buckling loads and postponing the initiation of damage and final structural failure. Also, thermally induced stresses due to curing cool-down have a great effect in increasing bifurcation loads. If the panels are notched at the centre, the difference to straight-fibre panels is even more remarkable. The numerical results show that the negative influence of a central hole on damage initiation and structural failure of a composite panel is reduced significantly if the panel is designed with of curvilinear overlapping tows instead of traditional straight-fibres.

Further damage analyses should make use of the correct IM7/8552 fracture energy values and take into account the wedge resin-rich regions created where tows are dropped. These may trigger damage initiation at a lower load stage. Also, the three-dimensional nature of overlapping tows should be fully described.

Acknowledgements

The funding of this research through the scholarship SFRH/BD/16238/2004 from the Portuguese Foundation for Science and Technology is gratefully acknowledged.

References

[1] Gürdal, Z. and Olmedo, R., "Composite Laminates with Spatially Varying Fiber Orientations: Variable Stiffness Panel Concept," Proceedings of the AIAA/ASME/ASCE/AHS/ASC 33rd Structures, Structural Dynamics and Materials Conference, Vol. 2, Dallas, TX, 1992, pp. 798–808, AIAA 92-2472.

[2] Gürdal, Z. and Olmedo, R., "In-Plane Response of Laminates with Spatially Varying Fiber Orientations: Variable Stiffness Concept," AIAA Journal , Vol. 31, No. 4, 1993, pp. 751–758.

[3] Olmedo, R. and Gürdal, Z., "Buckling Response of Laminates with Spatially Varying Fiber Orientations," Proceedings of the AIAA/ASME/ASCE/AHS/ASC 34rd Structures, Structural Dynamics and Materials Conference, La Jola, CA, April 1993, pp. 2261–2269, AIAA 93-1567.

[4] Waldhart, C., Gürdal, Z., and Ribbens, C., "Analysis of Tow Placed, Parallel Fiber, Variable Stiffness Laminates," Proceedings of the AIAA/ASME/ASCE/AHS/ASC 37rd Structures, Structural Dynamics and Materials Conference, Salt Lake City, UT, April 1996, pp. 2210–2220, AIAA 96-1569.

[5] Wu, K. and Gürdal, Z., "Thermal Testing of Tow-Placed, Variable Stiffness Panels," Proceedings of the AIAA/ASME/ASCE/AHS/ASC 42nd Structures, Structural Dynamics and Materials Conference, Seattle, WA, April 2001, AIAA 2001-1190.

[6] Wu, K., Gürdal, Z., and Starnes Jr., J., "Structural Response of Compression-Loaded, Tow-Placed, Variable Stiffness Panels," Proceedings of the AIAA/ASME/ASCE/AHS/ASC 43rd Structures, Structural Dynamics and Materials Conference, Denver, CO, April 2002, AIAA 2002-1512.

[7] Tatting, B. and Gürdal, Z., "Analysis and Design of Tow-Steered Variable Stiffness Composite Laminates," American Helicopter Society Hampton Roads Chapter, Structure Specialists' Meeting, Williamsburg, VA, October 2001.

[8] Tatting, B. and Gürdal, Z., "Design and Manufacture of Elastically Tailored Tow Placed Plates," Tech. rep., NASA, Langley Research Center, Hampton, VA, August 2002, NASA/CR-2002-211919.

[9] Lopes, C., Gürdal, Z., and Camanho, P., "Tow-Placed, Variable-Stiffness Composite Panels: Damage Tolerance Improvements over Traditional Straight-Fibre Laminates," III European Conference on Computational Mechanics: Solids, Structures Coupled Problems in Engineering, Lisbon, Portugal, June 2006.

[10] Pinho, S., Dávila, C., Camanho, P., Iannucci, L., and Robinson, P., "Failure Models and Criteria for FRP Under In-Plane or Three-Dimensional Stress States Including Shear Non-linearity," Tech. rep., NASA, Langley Research Center, Hampton, VA, February 2005, NASA/TM-2005-213530.

[11] Maimí, P., Camanho, P., Mayugo, J., and Dávila, C., "A Thermodynamically Consistent Damage Model for Advanced Composites," Tech. rep., NASA, Langley Research Center, Hampton, VA, March 2006, NASA/TM-2006-214282.

[12] Sleight, D., "Progressive Failure Analysis Methodology for Laminated Composite Structures," Tech. rep., NASA, Langley Research Center, Hampton, VA, March 1999, NASA/TP-1999-209107.

[13] Jegley, D., Tatting, B., and Gürdal, Z., "Optimization of Elastically Tailored Tow Placed Plates with Holes," Proceedings of the AIAA/ASME/ASCE/AHS/ASC 44th Structures, Structural Dynamics and Materials Conference, Norfolk, VA, April 2003, AIAA 2003-1420.

[14] Jegley, D., Tatting, B., and Gürdal, Z., "Tow-Steered Panels with Holes Subjected to Compression or Shear Loading," Proceedings of the AIAA/ASME/ASCE/AHS/ASC 46th Structures, Structural Dynamics and Materials (SDM) Conference, Austin, TX, April 2005, AIAA 2005-2017.

[15] Tavares, C., Fracture of Advanced Composite Materials: Experimental Basis for a Constitutive Model , Master's thesis, University of Porto, Porto, Portugal, January 2006.

[16] Camanho, P., Dávila, C., Pinho, S., Iannucci, L., and Robinson, P., "Prediction of in situ strengths and

matrix cracking in composites under transverse tension and in-plane shear," Composites Part A: Applied Science and Manufacturing, Vol. 1, No. 12, 2005.

[17] Tatting, B. and Gürdal, Z., "Automated Finite Element Analysis of Elastically-Tailored Plates," Tech. rep., NASA, Langley Research Center, Hampton, VA, December 2003, NASA/CR-2003-212679.